



## Wavelet-based super resolution using pansharpened multispectral images

Vildan ATALAY AYDIN<sup>1,\*</sup> , Hassan FOROOSH<sup>2</sup> 

<sup>1</sup>Computer Engineering, Faculty of Engineering, İzmir Demokrasi University, İzmir, Turkey

<sup>2</sup>Department of Computer Science, College of Engineering and Computer Science, University of Central Florida, Orlando, Florida, USA

Received: 24.09.2020

Accepted/Published Online: 10.02.2021

Final Version: 26.07.2021

**Abstract:** Several remote sensing applications require high-spatial-high-spectral resolution multispectral (MS) images. However, most MS sensors provide low-spatial-high-spectral resolution MS images together with high-spatial-low-spectral resolution panchromatic (PAN) bands. In order to increase the spatial resolution of MS bands to the resolution of PAN images and to obtain high-spatial/spectral resolution MS bands, either MS and PAN images are fused (i.e., pansharpening) or super resolution (SR) is performed using MS bands only. Nevertheless, existing methods do not utilize the available temporal and spatial information together. In this paper, we propose a multiframe SR algorithm using high-spatial/spectral resolution MS images (i.e., pansharpened), taking advantage of both spatial and temporal data, in order to exceed the spatial resolution of the available PAN bands. We first employ a wavelet-based pansharpening method on a set of MS and PAN images captured at different times. Then, we utilize these pansharpened MS bands in a wavelet-based multiframe SR scheme. The proposed method reveals the inter-wavelet-subband relationship of multitemporal images for SR. We demonstrate our results with comparisons on a Landsat 7 ETM+ dataset.

**Key words:** Super resolution, discrete wavelet transform, pansharpening

### 1. Introduction

In remote sensing imaging, spatial resolution indicates the ground area captured in one pixel; whereas, spectral resolution denotes the electromagnetic bandwidth of the signals [1]. Most multispectral (MS) sensors such as QuickBird, IKONOS, and Landsat 7 ETM+ capture a few bands, typically providing low-spatial-high-spectral resolution for the MS and high-spatial-low-spectral resolution for the panchromatic (PAN) images. However, several remote sensing applications, such as weather forecasting, change detection, map updating, and environmental monitoring require high-spatial/spectral resolution MS bands.

In order to obtain high-spatial resolution MS images, a large body of research is devoted to fuse information of MS and PAN bands, which is called pansharpening. The goal of pansharpening is to combine high frequency information of the PAN images with MS bands. Pansharpening methods can be categorized into five groups [1] as component substitution, relative spectral contribution, high-frequency injection, image statistics-based, and multiresolution. Most pansharpening techniques upsample the MS bands to the size of PAN ones as a first step. After the upsampling step, component substitution based methods [2, 3] transform the MS bands, perform histogram matching on MS bands and PAN images and substitute components of MS with the PAN bands. These methods perform backward transform on the substituted components as a final step. Relative

\*Correspondence: vildan.atalayaydin@idu.edu.tr

spectral contribution methods [4] employ a linear combination of bands instead of using substitution after the histogram matching step. Methods in the high-frequency injection group [5] apply a low-pass filter to the PAN image, and find the difference between the original and filtered PAN images (i.e. high-frequency information). This difference is then added to the MS bands to obtain the pansharpened ones. Image statistics based models [6] use the statistical relationship between each band of the MS and PAN images generally using the Bayesian approach. Finally, multiresolution methods can also be categorized into two sets as Laplacian pyramid and wavelet-based. Laplacian pyramid based methods [7] find the pyramid for the PAN image, and add the details from the pyramid to the MS bands after determining weights for the pyramid coefficients. Moreover, wavelet-based methods [8, 9] perform forward transform on MS and PAN images, apply fusion on the coefficients in the transform domain, and finally perform inverse transform.

Pansharpening methods do not take advantage of the temporal information captured by the MS sensors. On the other hand, multiframe super resolution (SR) methods, in general, are used to fuse a sequence of degraded or aliased low resolution (LR) images of the same scene that can be taken at different times, to obtain a high resolution (HR) image. Approaches to solve the SR problem can be classified into interpolation, regularization, learning-based, and frequency domain methods [10]. Interpolation-based methods [11, 12] fuse information from all LR images using a general interpolation technique (e.g., nearest neighbor, bilinear, bicubic). To stabilize the ill-posedness of SR problem, regularization-based methods [13] optimize a cost function with a regularization term by incorporating prior knowledge. Learning-based methods [14] obtain an HR image from generally a single image by utilizing training sets of LR/HR images. Frequency domain methods can be categorized into two groups as Fourier and wavelet domain techniques. Fourier-based methods [15, 16] use the aliasing property of LR images. Wavelet-based SR techniques [15, 17, 18], on the other hand, use the LR images to model the lowpass subbands of an unknown HR image. This assumption allows reconstruction of the high frequency information of the HR image, which is lost during image acquisition.

To incorporate SR methodology into remote sensing, and to take advantage of the temporal information provided by MS sensors, Li *et al.* [19] propose a wavelet-based multiframe SR technique, where temporal information of low-spatial-resolution MS images are used to increase their spatial resolution. The authors propose using an SR method based on maximum a posteriori (MAP) framework with a universal hidden Markov tree model as a preprocessing step for MS image classification. SR is applied band-by-band to MS images captured on different dates. However, although their method uses the temporal information, it does not take the available high-spatial resolution PAN image into account.

In this paper, we propose a wavelet-based multiframe SR method that takes advantage of both temporal and spatial information captured by MS sensors, in order to obtain a high spatial resolution MS image, which exceeds the spatial resolution of the PAN image while keeping the high-spectral resolution. To achieve this goal, we first apply a wavelet-based pansharpening method to a set of MS and corresponding PAN images taken at different times, to obtain high-spatial resolution (i.e., pansharpened) MS images. We then propose a wavelet-based approach for SR which is applied band-by-band on the pansharpened MS images, in order to achieve a higher spatial resolution MS image. For the proposed SR method, we assume that pansharpened MS images (i.e. LR) correspond to the approximation coefficients of the first level discrete wavelet transform (DWT) of unknown higher spatial resolution MS images (i.e. HR). For the SR process, we use the closed-form expressions derived by Aydin and Foroosh [20] where the relationship between high frequency information of the reference HR image and low frequency information in the given sequence of LR views is defined. We then solve the SR

problem in a modified iterative back projection (IBP) manner.

The remainder of this paper is organized as follows. In Section 2, a brief summary of related research is provided. In Section 3, the pansharpening method utilized in this paper and the proposed approach for SR are presented. In Section 4, the experimental results and comparisons are demonstrated. Finally, discussion and concluding remarks are provided in Section 5.

## 2. Related work

In this section, we overview the pansharpening techniques and wavelet-based SR methods. We also address the use of SR in remote sensing.

One of the pioneering methods in component substitution group is the Intensity-Hue-Saturation (IHS) pansharpening [21], which utilizes the IHS color space. Later, this method is enhanced to decrease the spectral distortion [2]. Gram–Schmidt (GS) spectral sharpening [3] can be put in the component substitution group, as well, where Gram–Schmidt method is used to reduce the redundancy in MS bands. The Brovey transform [4] is one of the classical methods in relative spectral contribution group, which uses chromaticity transform. One of the works in high-frequency injection group is proposed by Chavez and Pat [22], where high-frequency information is extracted from the PAN image using a high-pass filter and injected into the MS bands. High-frequency modulation method [5] performs injection of high-frequency information using a modulation coefficient [1]. Another group of pansharpening methods focuses on the statistical properties of MS bands and PAN images. One of the first works in this group is proposed by Price [6], where a linear model is used to obtain the statistical relationship between low-spatial resolution MS, high-spatial resolution PAN, and high-spatial resolution MS bands. In addition, Fasbender *et al.* [23] propose a pansharpening method based on the Bayesian framework, where the statistical relationship between MS and PAN images are used in a weighted scheme, in order to match the user needs. Finally, wavelet-based methods include the works by Kim *et al.* [8] where an improved additive-wavelet fusion method is proposed using the à trous algorithm, which does not decompose the MS image to preserve the radiometric data, and Otazu *et al.* [24] who propose a wavelet-based method that incorporates the 'physical electromagnetic spectrum responses of sensors' in order to suppress the artifacts. Garzelli and Nencini [7] model the relationship between the wavelet coefficients of MS bands and PAN images at a coarser resolution, and later use this relationship to estimate the high-spatial resolution MS bands. Alparone *et al.* [25] compare several pansharpening methods and conclude that the multiresolution based ones and the methods that employ adaptive models for the injection of highpass details outperform all the others.

We can summarize the wavelet-based SR approaches, as follows. Robinson *et al.* [15] apply a combined Fourier-wavelet deconvolution and denoising algorithm to multiframe SR, in order to reduce noise in SR methods. On the other hand, to reduce degradation artifacts such as blurring and the ringing effect, Temizel and Vlachos [26] utilize zero padding in the wavelet domain followed by cycle spinning. For deblurring, Chan *et al.* [27] derive iterative algorithms, which decompose HR image obtained from an iteration into different frequency components and add them to the next iteration. Jiji *et al.* [28], as an example to learning-based methods, handle the problem of representing the relationship between LR/HR frames by training their dataset with HR images by learning from wavelet coefficients at finer scales, followed by regularization in a least squares manner

SR methods are also widely utilized for remote sensing. Demirel and Anbarjafari [17] use DWT and an intermediate stage for estimating high frequency information for satellite image super resolution. Patel and Joshi [29] propose a learning-based approach for SR of hyperspectral images using the DWT, where application-

specific wavelet basis (i.e. filter coefficients) are designed. Moreover, Zhang *et al.* [30] propose a MAP-based multiframe SR method for hyperspectral images, where principle component analysis is employed in order to reduce the computational complexity. A comprehensive review on single-frame SR techniques for remote sensing applications is provided by Fernandez–Beltran *et al.* [31].

### 3. Super resolution of pansharpened multispectral images

In this section, we will explain the employed pansharpening method and the proposed super resolution technique.

#### 3.1. Pansharpening

We choose additive wavelet luminance proportional (AWLP) [24] method for the pansharpening step of our algorithm, based on the comparisons by Alparone *et al.* [25] and Bovolo *et al.* [32].

The AWLP method is an extended version of the additive wavelet luminance technique (AWL), which is designed for three-band (RGB) multispectral images and works in the IHS domain. This method injects high frequency information of the PAN image to MS images proportional to their original values in order to preserve the radiometric signature of MS images. The AWLP method generalizes the AWL method to include arbitrary number of bands, as in the formula below:

$$A_{P_i} = A_i + \frac{A_i}{\sum_{i=1}^L A_i} \sum_{j=1}^n w(P), \tag{1}$$

where  $A$  and  $A_P$  are low resolution and pansharpened MS bands, and  $P$  shows the PAN image, respectively.  $L$  is the number of MS bands,  $w$  is the Discrete Wavelet Transform decomposition, and  $n$  is the number of DWT levels. Pansharpening step (for four sets of MS and PAN bands) is demonstrated in Figure 1.

#### 3.2. Super resolution

General SR observation model can be described as follows:

$$\mathbf{a}_k = \mathbf{\Lambda}_k \mathbf{M}_k \mathbf{B}_k \mathbf{i} + \mathbf{n}_k, \tag{2}$$

where  $\mathbf{a}_k$  shows the observed LR images, and  $\mathbf{i}$  demonstrates the unknown HR image in lexicographical order.  $\mathbf{\Lambda}$ ,  $\mathbf{M}$ ,  $\mathbf{B}$ , and  $\mathbf{n}$  indicate downsampling, motion, blur, and noise for each LR image. Subscript  $k$  indicates the number of images in the LR set, for  $k = 1, \dots, K$ . Throughout the paper, uppercase bold letters indicate matrices; whereas, lowercase bold ones show vectors.

Since our goal is to increase the available spatial resolution of PAN images while keeping the spectral resolution provided by MS bands, we propose using temporal, spectral, and spatial information accessible via most MS sensors. In order to achieve our goal, we use pansharpened MS images as LR images in the general SR scheme.

Now, we can update the SR observation model to use the pansharpened MS images, as follows:

$$\mathbf{a}_{P_{i,k}} = \mathbf{\Lambda} \mathbf{M}_{i,k} \mathbf{B}_{i,k} \mathbf{i} + \mathbf{n}_{i,k}, \tag{3}$$

where  $\mathbf{a}_P$  shows the pansharpened MS images (i.e., the observed LR images in Eq. (2)) and  $\mathbf{i}$  demonstrates the desired HR MS image (i.e., the unknown HR image in Eq. (2)), in lexicographical order.  $\mathbf{\Lambda}$ ,  $\mathbf{M}$ ,  $\mathbf{B}$ , and  $\mathbf{n}$

indicate downsampling (assuming same scale for all images), motion, blur, and noise, as before, and subscript  $i$  indicates the number of bands, for  $i = 1, \dots, L$ . Figure 1 shows a pictorial explanation of the proposed method.

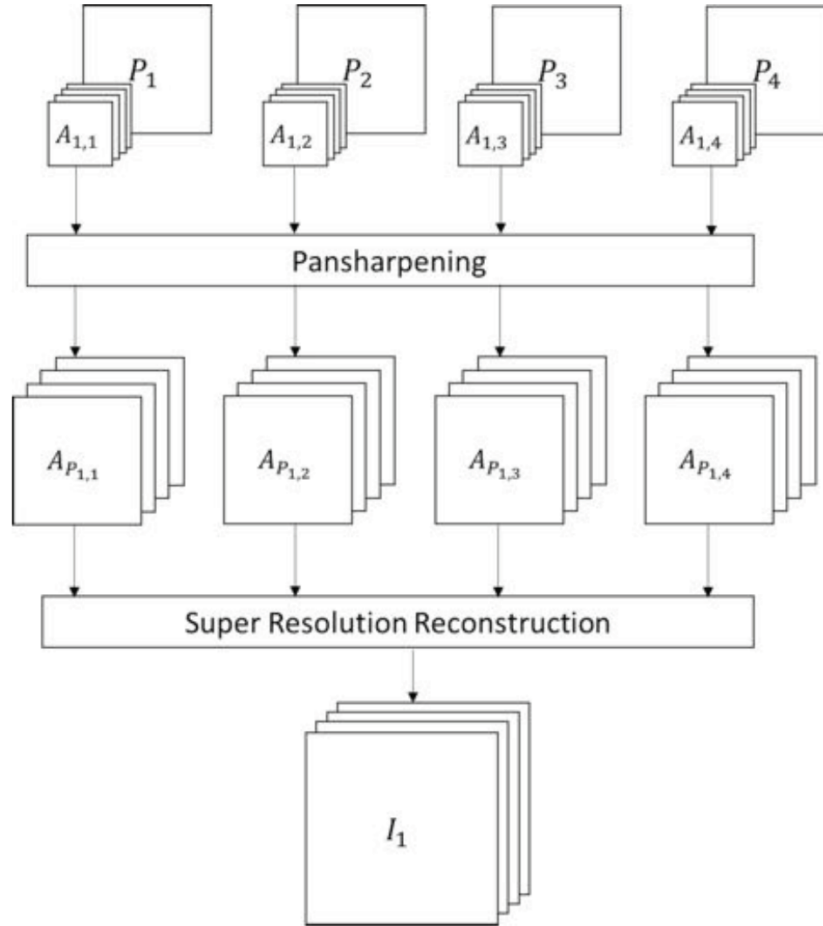


**Figure 1.** Flowchart of the proposed method for super resolution of pansharpened multispectral images.

We assume that the pansharpened MS bands ( $\mathbf{a}_P$  in Eq. (3) and  $A_P$  in Figure 1) are the lowpass subbands of DWT of unknown HR MS bands ( $\mathbf{i}$  in Eq. (3) and  $I$  in Figure 1). The goal is to reconstruct the unknown highpass subbands of these HR MS bands. We can write the iterative procedure to reconstruct the unknown information as follows:

$$\mathbf{I}_i^{n+1} = \mathbf{I}_i^n + \lambda \sum_k (\mathbf{A}_{P_{i,k}} - \hat{\mathbf{A}}_{P_{i,k}}) \mathbf{h}^{\text{BP}}, \quad (4)$$

where  $\hat{\mathbf{A}}_P$ ,  $\lambda$ , and  $\mathbf{h}^{\text{BP}}$  show estimated pansharpened MS images, regularization parameter, backprojection kernel in the iterative back projection based SR technique, proposed first by Irani and Peleg [11], respectively. Superscript  $n$  demonstrates the iteration number. We can rewrite the above formula using Eq. (1), as follows;

$$\mathbf{I}_i^{n+1} = \mathbf{I}_i^n + \lambda \sum_k \left\{ \left( \mathbf{A}_{i,k} + \frac{\mathbf{A}_{i,k}}{\sum_{i=1}^L \mathbf{A}_{i,k}} \sum_{j=1}^n w(\mathbf{P})_k \right) - \text{tr}(\mathbf{X}_i) \right\} \mathbf{h}^{\text{BP}}, \quad (5)$$

where  $\text{tr}$  denotes the trace of  $\mathbf{X}$ . Eq. (5) shows the relationship between the low-spatial resolution MS bands ( $\mathbf{A}$ ), PAN images ( $\mathbf{P}$ ), and the unknown higher-spatial resolution MS bands ( $\mathbf{I}$ ) that we want to recover. We define  $\mathbf{X}$ , based on the derivations by Aydin and Foroosh [20], as follows:

$$\mathbf{X} = \begin{bmatrix} \mathbf{F}_{y_k} & & & \\ & \mathbf{F}_{y_k} & & \\ & & \mathbf{K}_{y_k} & \\ & & & \mathbf{K}_{y_k} \end{bmatrix} \begin{bmatrix} \mathbf{A}_{i,1} + \frac{\mathbf{A}_{i,1}}{\sum_{i=1}^L \mathbf{A}_{i,1}} \sum_{j=1}^n w(\mathbf{P}_j) & & & \\ & \hat{\mathbf{H}}^n & & \\ & & \hat{\mathbf{V}}^n & \\ & & & \hat{\mathbf{D}}^n \end{bmatrix} \begin{bmatrix} \mathbf{F}_{x_k} & & & \\ & \mathbf{K}_{x_k} & & \\ & & \mathbf{F}_{x_k} & \\ & & & \mathbf{K}_{x_k} \end{bmatrix} \quad (6)$$

Eq. (6) demonstrates the calculation of pansharpened estimates ( $\hat{\mathbf{A}}_{P_{i,k}}$ ), for  $k = 2, \dots, K$ , by using a reference image (i.e.,  $\mathbf{A}_{i,1}$ ) and wavelet transform horizontal, vertical, and diagonal subbands (i.e.,  $\mathbf{H}, \mathbf{V}, \mathbf{D}$ ) using the methodology derived by Aydin and Foroosh [20], assuming the reference image corresponds to the approximation subband of the wavelet transform. Here, the displacements between images are assumed to be subpixel, and matrices,  $\mathbf{F}_x$  and  $\mathbf{K}_x$  are defined, as follows;

$$\mathbf{F}_x = \frac{1}{2^{\ell_x+1}} \begin{bmatrix} 2^{\ell_x+1} - |s_x| & & & & & \\ & |s_x| & & & & \\ & & 2^{\ell_x+1} - |s_x| & & & \\ & & & |s_x| & & \\ & & & & \ddots & \ddots \\ & & & & & |s_x| & & 2^{\ell_x+1} - |s_x| \end{bmatrix},$$

$$\mathbf{K}_x = \frac{1}{2^{\ell_x+1}} \begin{bmatrix} -s_x & & & & & \\ s_x & -s_x & & & & \\ & s_x & & & & \\ & & \ddots & \ddots & & \\ & & & & s_x & -s_x \end{bmatrix}$$

where  $s_x$  and  $\ell_x$  demonstrate integer shift amount and the number of wavelet transform levels to be added to the original images to reach the integer shift amount, for  $x$  direction.  $\mathbf{F}_x$  and  $\mathbf{K}_x$  are of size  $n \times n$ , while  $\mathbf{F}_y$  and  $\mathbf{K}_y$  are the matrices used for  $y$  direction, and of size  $m \times m$ . Derivations are explained more in detail in Aydin and Foroosh [20]. The matrices for  $y$  direction are defined in the same manner.

SR process consists of two parts as image registration and image reconstruction. Since satellite images are assumed to have only translational shifts between them, we generalize the in-band (i.e., in the wavelet domain) subpixel shift method by Aydin and Foroosh [33] to pixel level shifts. We first perform full search for pixel accuracy, by using the in-band shift method by Aydin and Foroosh [34], which use the same inter-subband relationship defined above in Eq. (6). In order to decrease the computational complexity, we divide the search into two steps. First, full search for every five pixels is performed. The result obtained in the first step is later

refined to pixel accuracy with full search for every pixel, in a  $[-5, 5]$  range. Finally, we perform the subpixel registration method by Aydin and Foroosh [33].

Since we assume that MS image bands captured by the same sensor are already aligned, we perform registration between MS images taken at different dates, on one band only, and apply the same registration parameters to all bands. We perform the proposed SR scheme on each band of multitemporal pansharpened MS images.

The proposed algorithm can also be explained step by step as in **Algorithm** - super resolution using pansharpened MS images.

**Algorithm** *SR using pansharpened MS images*

- *Input*: Multitemporal MS and PAN bands
- *Objective*: Obtain high resolution MS images, exceeding the PAN band spatial resolution
- *Output*: High-spatial/high-spectral resolution MS images
- ▶ Pansharpening
  - ◊ Perform AWLP pansharpening, on a set of MS bands and PAN images, taken at different dates
- ▶ Super resolution
  - ◊ Image registration
    - \* Register the first band of all target images to the first band of reference pansharpened image
  - ◊ Image reconstruction (do for all bands)
    - \* Initialize high-frequency information for the unknown HR image
    - \* Construct coefficient matrices ( $\mathbf{F}$  and  $\mathbf{K}$ ) for all LR images, using registration parameters found for translation
    - \* Until a predefined number of maximum iterations, do:
      - Use wavelet subbands with constructed matrices to estimate LR images ( $\hat{\mathbf{A}}_P$ ), using Eq. (6)
      - Update HR image ( $\mathbf{I}$ ), using Eq. (5)

In the next section, experimental results on both simulated and real dataset will be demonstrated.

#### 4. Experimental results

We test our proposed method using Landsat 7 ETM+ images, which have seven MS bands together with a PAN band. The spectral resolution of MS bands range from  $0.45\mu\text{m}$  to  $2.35\mu\text{m}$ , while PAN bands span  $0.52-0.9\mu\text{m}$  spectrum; and, the spatial resolution of MS bands are 30 m, whereas PAN bands are 15 m. We select four multispectral image groups together with their PAN bands from a region in İstanbul, Turkey, captured on July 2, September 4 in 2000 and May 18, August 6 in 2001, for which the pansharpened versions are shown in Figure 2 (Images are courtesy of USGS Glovis). We conduct two sets of tests which are categorized as simulated and real experiments. All tests are carried after MS and PAN bands are fused in the pansharpening step.

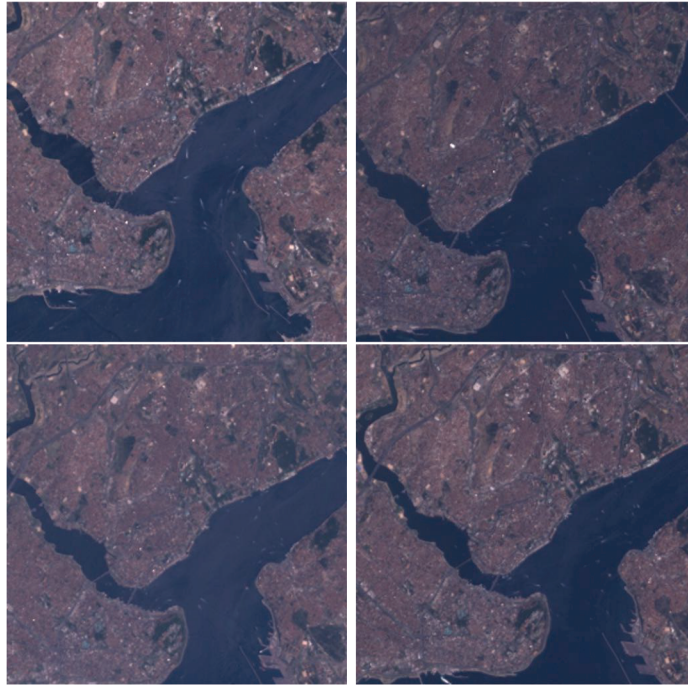


**Figure 2.** Real pansharpened MS images (RGB bands only).

#### 4.1. Simulated dataset

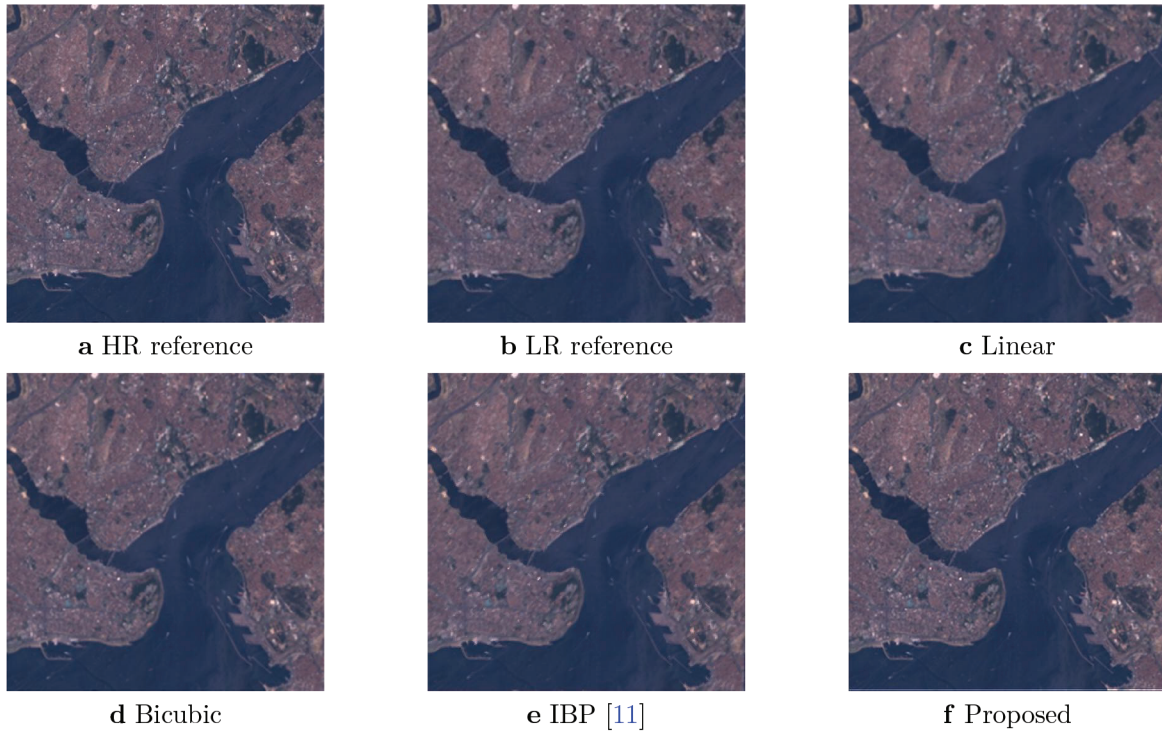
Since there is no ground truth for the proposed method, first test is a simulated experiment where one of the pansharpened MS images is chosen as reference, all its bands are shifted in horizontal, vertical, and diagonal directions for one pixel, convolved with a Gaussian filter, and downsampled, which is a conventional method used for simulated SR experiments [30]. The pansharpened MS image bands chosen as reference is then used as the ground truth in comparisons.

For image registration, one of the bands of the reference pansharpened MS image is chosen as the reference band, and image registration is performed for the same band of all other groups of images. The proposed in-band method is defined using subpixel displacements between images; therefore, image regions are adjusted after the registration step, in order for all images to cover the same area. We then initialize our HR estimate using the inverse wavelet transform on known reference LR and upsampled wavelet subbands (i.e., wavelet subband estimations) of this LR image. The iterative method described in Section 3.2 is then applied in order to estimate the reconstructed HR image. We compare our results both qualitatively and quantitatively with conventional interpolation techniques and the iterative back projection (IBP) method [11], since the proposed method is a modified IBP model. All compared methods are given the same pansharpened MS images, and the registration parameters as input, if needed. Quantitative comparisons are based on Peak-Signal-to-Noise-Ratio (PSNR) and Structural Similarity Index (SSIM) [35].

All figures for simulated and real experiments show a composite of R, G, and B bands. Figure 3 shows reference HR and reference LR images together with the compared methods including Bilinear interpolation, Bicubic interpolation and IBP method. In order to comprehend the results, Figures 4 and 5 provide zoomed areas of all images in Figure 3. As can be seen from these figures, the proposed method preserves spectral information of the MS bands while increasing the spatial resolution. Comparisons of the figures confirm that



the proposed method reconstructs edges better than the compared ones, while preventing ringing artifacts as in the compared IBP method.



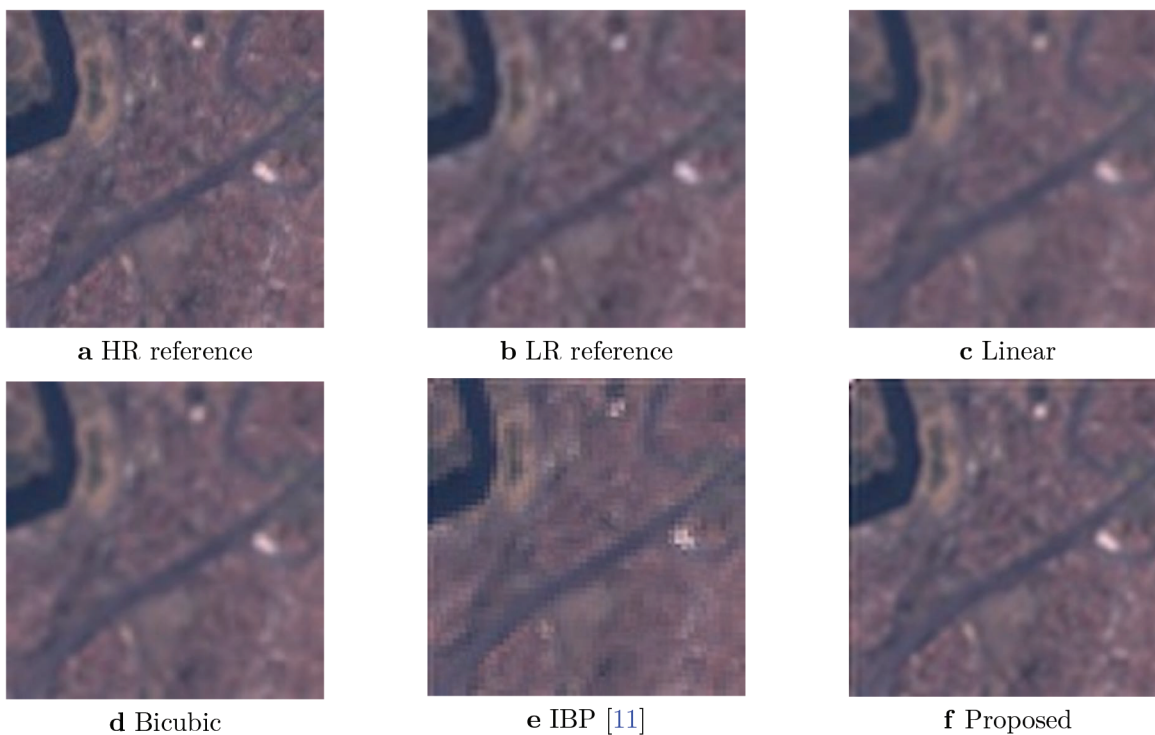
**Figure 3.** Simulated dataset comparison.

Table 1 demonstrates the results based on PSNR and SSIM values for each band, for a resolution enhancement factor of two. Since pansharpening methods use MS bands numbered 1, 2, 3, 4, 5, and 7 for Landsat 7 ETM+, we compare the results for these bands. Quantitative comparisons also validate the qualitative ones. In general, the proposed method preserves the spectral information better while increasing the spatial resolution.

**Table 1.** Comparison of proposed method with other methods in PSNR and SSIM.

Band	Linear		Bicubic		IBP		Proposed	
	PSNR	SSIM	PSNR	SSIM	PSNR	SSIM	PSNR	SSIM
1	32.47	0.87	34.12	0.90	27.62	0.72	<b>37.08</b>	<b>0.95</b>
2	34.61	0.92	36.71	0.95	29.51	0.82	<b>40.21</b>	<b>0.97</b>
3	36.15	0.93	38.22	0.95	31.54	0.84	<b>41.70</b>	<b>0.98</b>
4	33.20	0.94	35.04	0.96	27.04	0.85	<b>37.88</b>	<b>0.98</b>
5	31.79	0.81	33.23	0.85	27.03	0.64	<b>35.88</b>	<b>0.92</b>
7	32.49	0.85	34.23	0.89	27.41	0.69	<b>37.21</b>	<b>0.94</b>

Since pansharpening and image registration methodologies are performed once for our experiments, and the results of these techniques are utilized for all compared super resolution methods when needed, we examine the computational complexity for the proposed super resolution method only. Time complexity of the image registration model can be found in [33]. The computational complexity of the proposed method is determined



**Figure 4.** Zoomed areas of simulated dataset results in Figure 3.

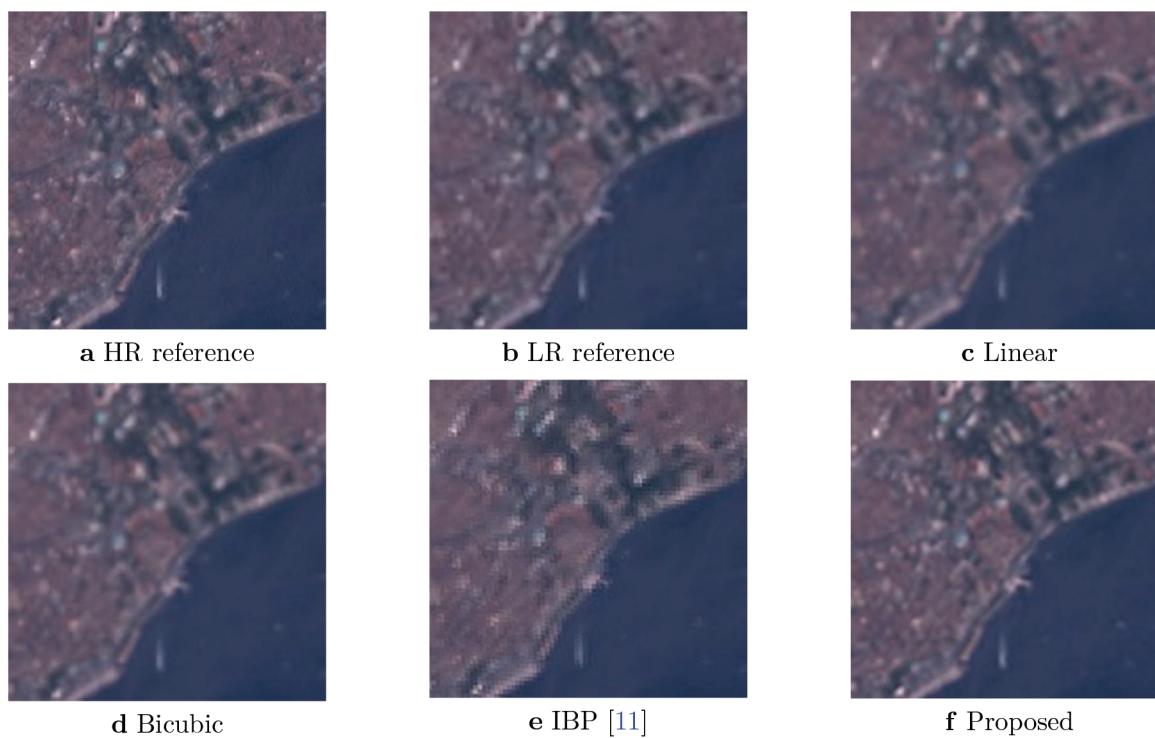


**Figure 5.** Zoomed areas of simulated dataset results in Figure 3.

by the matrix multiplications in Eq. (6); therefore, the complexity of the proposed algorithm is  $O(m^2n^2)$ , where  $m$  and  $n$  are the size of LR images in  $x$  and  $y$  directions. We compare the average time taken by the proposed method and the compared ones. The time taken by the proposed method is 26.46 seconds (s), while IBP method is 6.003 s, nearest neighbor interpolation is 0.003 s, linear interpolation is 0.005 s, and bicubic interpolation is 0.007 s. The time taken by the proposed super resolution method can be tolerated since the proposed algorithm outperforms the compared ones in resolution quality based on the qualitative and quantitative results, as discussed above.

#### 4.2. Real dataset

For the second test, we use pansharpened MS bands as our LR image set, and estimate an HR image without a ground truth; where we compare the results qualitatively. Figure 2 shows the real dataset used for the experiments.

Figure 6 demonstrates the reconstruction results obtained by Nearest Neighbor, Bilinear and Bicubic interpolation, IBP method, and the proposed model. When ground area changes over time (e.g., in Figure 2, caused by the ships), the accuracy of SR decreases due to the fact that multitemporal images are fused. The zoomed subregions in Figures 7 and 8 of the results in Figure 6 demonstrate the reconstruction details better since these areas have mostly constructions and forests with the least change during the used time period.

Experiments with the real dataset also approve the ones with the simulated ones. One can see that the edges of roads and constructions in Figure 6 (f) are well reconstructed. As seen in the zoomed areas in Figures 7 and 8, proposed method smoothes jaggy artifacts, generates sharper edges while keeping the spectral information at the same time.

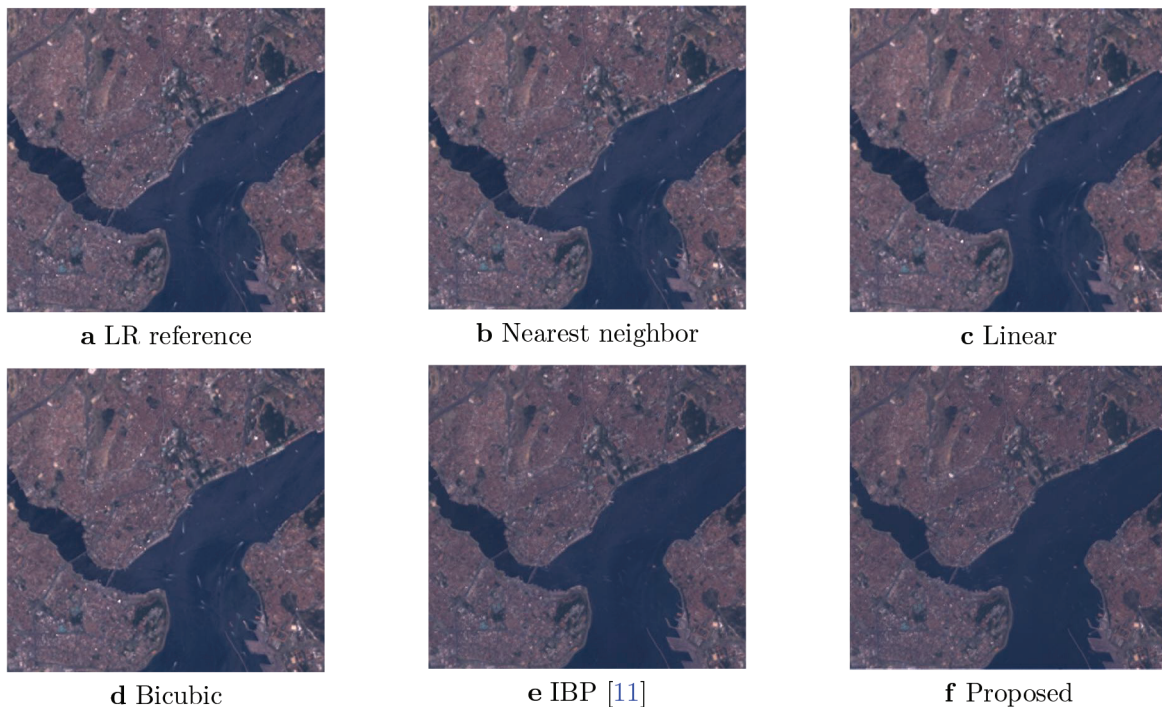


**Figure 6.** Real dataset results comparison.

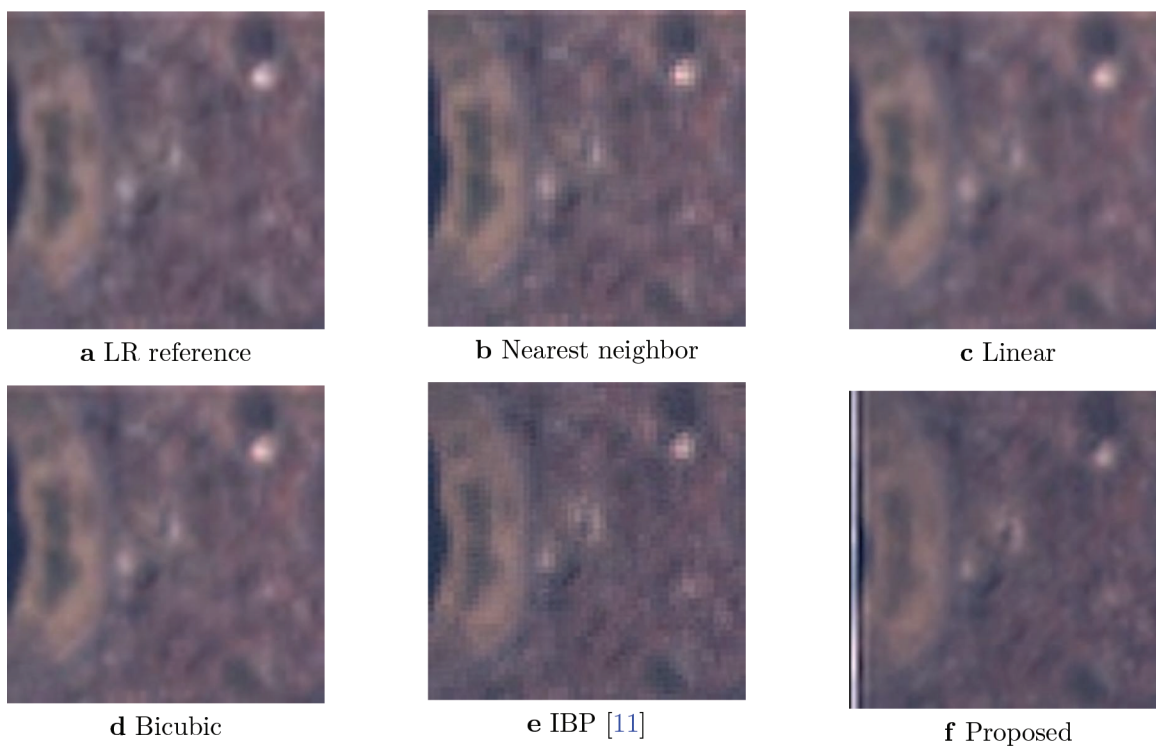


Figure 7. Zoomed areas of real dataset results in Figure 6.

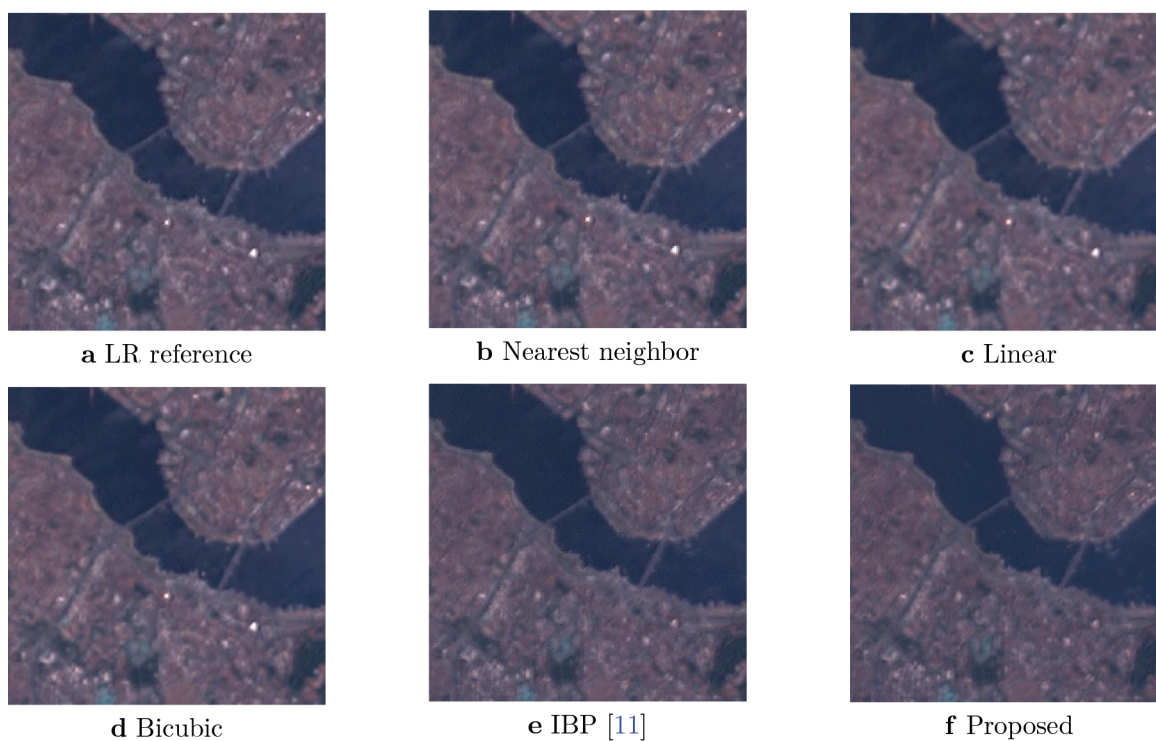


Figure 8. Zoomed areas of real dataset results in Figure 6.

## 5. Discussion and Conclusion

Several multispectral satellite imaging applications require high-spatial/spectral resolution MS images; yet, most MS sensors provide high-spectral-resolution MS and high-spatial-resolution PAN images, separately. Methods used to increase the spatial resolution of MS bands either use the spatial information of PAN images in pansharpening or the multitemporal data in MS bands in super resolution. Our goal is to exceed the resolution of available PAN images provided by the sensors, to reach a higher resolution that could be captured by different sensors, in a more costly manner. Therefore, in this paper, we propose employing pansharpening and SR methods together, to exceed the spatial resolution in the PAN bands, by using both spatial and temporal data captured by multispectral sensors. Experimental results conducted on real datasets captured by Landsat 7 ETM+ satellite demonstrate that the proposed method reconstructs details as well as keeps the spectral information. The findings of this study suggest that wavelet-based pansharpening and super resolution methods performed in satellite imagery have encouraging results. The proposed model has promising results based on quality; however, it requires higher runtime compared to the other methods due to the fact that matrix multiplications are performed in the super resolution step; therefore, further research focused on the computational cost of the algorithm should be undertaken. Another possible area of future work is to explore the reconstruction of nonstationary objects using single image super resolution techniques. The main goal of the present study is to exceed the spatial resolution of the available PAN images provided by satellites. The results obtained in this study will be of interest to many remote sensing applications that require high-spatial/spectral resolution, such as map updating and change detection since more detailed remotely sensed images are obtained by using the already available information provided by sensors.

## References

- [1] Amro I, Mateos J, Vega M, Molina R, Katsaggelos AK. A survey of classical methods and new trends in pansharpening of multispectral images. *EURASIP Journal on Advances in Signal Processing* 2011; 2011 (1): 1-22. doi: 10.1186/1687-6180-2011-79
- [2] Tu TM, Huang PS, Hung CL, Chang CP. A fast intensity-hue-saturation fusion technique with spectral adjustment for IKONOS imagery. *IEEE Geoscience and Remote Sensing Letters* 2004; 1 (4): 309-312. doi: 10.1109/LGRS.2004.834804
- [3] Laben CA, Brower BV, inventors; Eastman Kodak Co, assignee. Process for enhancing the spatial resolution of multispectral imagery using pan-sharpening. United States Patent US 6,011,875. 2000 Jan 4.
- [4] Gillespie AR, Kahle AB, Walker RE. Color enhancement of highly correlated images. II. Channel ratio and "chromaticity" transformation techniques. *Remote Sensing of Environment* 1987; 22 (3): 343-365. doi: 10.1016/0034-4257(87)90088-5
- [5] Schowengerdt RA. *Remote sensing: models and methods for image processing*. Elsevier, 2006.
- [6] Price JC. Combining multispectral data of differing spatial resolution. *IEEE Transactions on Geoscience and Remote Sensing* 1999; 37 (3): 1199-1203. doi: 10.1109/36.763272
- [7] Garzelli A, Nencini F. Interband structure modeling for pan-sharpening of very high-resolution multispectral images. *Information Fusion* 2005; 6 (3): 213-224. doi: 10.1016/j.inffus.2004.06.008
- [8] Kim Y, Lee C, Han D, Kim Y, Kim Y. Improved additive-wavelet image fusion. *IEEE Geoscience and Remote Sensing Letters* 2010; 8 (2): 263-7. doi: 10.1109/LGRS.2010.2067192
- [9] Delleji T, Kallel A, Ben Hamida A. Multispectral image adaptive pansharpening based on wavelet transformation and NMDB approaches. *International Journal of Remote Sensing* 2014; 35 (19): 7069-7098. doi: 10.1080/01431161.2014.967883

- [10] Tian J, Ma KK. A survey on super-resolution imaging. *Signal, Image and Video Processing* 2011; 5 (3): 329-42. doi: 10.1007/s11760-010-0204-6
- [11] Irani M, Peleg S. Improving resolution by image registration. *CVGIP: Graphical Models and Image Processing* 1991; 53 (3): 231-239. doi: 10.1016/1049-9652(91)90045-L
- [12] Zhou F, Yang W, Liao Q. Interpolation-based image super-resolution using multisurface fitting. *IEEE Transactions on Image Processing* 2012; 21 (7): 3312-3318. doi: 10.1109/TIP.2012.2189576
- [13] Babacan SD, Molina R, Katsaggelos AK. Variational Bayesian super resolution. *IEEE Transactions on Image Processing* 2010; 20 (4): 984-999. doi: 10.1109/TIP.2010.2080278
- [14] Wang Z, Yang Y, Wang Z, Chang S, Han W et al. Self-tuned deep super resolution. In: *IEEE 2015 Conference on Computer Vision and Pattern Recognition Workshops*; Boston, Massachusetts, USA; 2015. pp. 1-8. doi: 10.1109/CVPRW.2015.7301266
- [15] Robinson MD, Toth CA, Lo JY, Farsiu S. Efficient Fourier-wavelet super-resolution. *IEEE Transactions on Image Processing* 2010; 19 (10): 2669-81. doi: 10.1109/TIP.2010.2050107
- [16] Vandewalle P, Sbaiz L, Vandewalle J, Vetterli M. Super-resolution from unregistered and totally aliased signals using subspace methods. *IEEE Transactions on Signal Processing* 2007; 55 (7): 3687-3703. doi: 10.1109/TSP.2007.894257
- [17] Demirel H, Anbarjafari G. Discrete wavelet transform-based satellite image resolution enhancement. *IEEE Transactions on Geoscience and Remote Sensing* 2011; 49 (6): 1997-2004. doi: 10.1109/TGRS.2010.2100401
- [18] Dong W, Zhang L, Shi G, Wu X. Image deblurring and super-resolution by adaptive sparse domain selection and adaptive regularization. *IEEE Transactions on Image Processing* 2011; 20 (7): 1838-1857. doi: 10.1109/TIP.2011.2108306
- [19] Li F, Jia X, Fraser D. Superresolution reconstruction of multispectral data for improved image classification. *IEEE Geoscience and Remote Sensing Letters* 2009; 6 (4): 689-693. doi: 10.1109/LGRS.2009.2023604
- [20] Aydin VA, Foroosh H. A linear well-posed solution to recover high-frequency information for super resolution image reconstruction. *Multidimensional Systems and Signal Processing* 2018; 29 (4): 1309-1330. doi: 10.1007/s11045-017-0499-3
- [21] Carper W, Lillesand T, Kiefer R. The use of intensity-hue-saturation transformations for merging SPOT panchromatic and multispectral image data. *Photogrammetric Engineering and Remote Sensing* 1990; 56 (4): 459-467.
- [22] Chavez Jr PS. Digital merging of Landsat TM and digitized NHAP data for 1: 24 000-scale image mapping. *Photogrammetric Engineering and Remote Sensing* 1986; 52 (10): 1637-1646.
- [23] Fasbender D, Radoux J, Bogaert P. Bayesian data fusion for adaptable image pansharpening. *IEEE Transactions on Geoscience and Remote Sensing* 2008; 46 (6): 1847-1857. doi: 10.1109/TGRS.2008.917131
- [24] Otazu X, González-Audícana M, Fors O, Núñez J. Introduction of sensor spectral response into image fusion methods. Application to wavelet-based methods. *IEEE Transactions on Geoscience and Remote Sensing* 2005; 43 (10): 2376-2385. doi: 10.1109/TGRS.2005.856106
- [25] Alparone L, Wald L, Chanussot J, Thomas C, Gamba P et al. Comparison of pansharpening algorithms: Outcome of the 2006 GRS-S data-fusion contest. *IEEE Transactions on Geoscience and Remote Sensing* 2007; 45 (10): 3012-3021. doi: 10.1109/TGRS.2007.904923
- [26] Temizel A, Vlachos T. Wavelet domain image resolution enhancement using cycle-spinning. *Electronics Letters* 2005; 41 (3): 119-121. doi: 10.1049/el:20057150
- [27] Chan RH, Chan TF, Shen L, Shen Z. Wavelet algorithms for high-resolution image reconstruction. *SIAM Journal on Scientific Computing* 2003; 24 (4): 1408-1432. doi: 10.1137/S1064827500383123
- [28] Jiji CV, Joshi MV, Chaudhuri S. Single-frame image super-resolution using learned wavelet coefficients. *International Journal of Imaging Systems and Technology* 2004; 14 (3): 105-112. doi: 10.1002/ima.20013

- [29] Patel RC, Joshi MV. Super-resolution of hyperspectral images: Use of optimum wavelet filter coefficients and sparsity regularization. *IEEE Transactions on Geoscience and Remote Sensing* 2014; 53 (4): 1728-1736. doi: 10.1109/TGRS.2014.2346811
- [30] Zhang H, Zhang L, Shen H. A super-resolution reconstruction algorithm for hyperspectral images. *Signal Processing* 2012; 92 (9): 2082-2096. doi: 10.1016/j.sigpro.2012.01.020
- [31] Fernandez-Beltran R, Latorre-Carmona P, Pla F. Single-frame super-resolution in remote sensing: a practical overview. *International Journal of Remote Sensing* 2017; 38 (1): 314-354. doi: 10.1080/01431161.2016.1264027
- [32] Bovolo F, Bruzzone L, Capobianco L, Garzelli A, Marchesi S et al. Analysis of the effects of pansharpening in change detection on VHR images. *IEEE Geoscience and Remote Sensing Letters* 2009; 7 (1): 53-7. doi: 10.1109/LGRS.2009.2029248
- [33] Aydin VA, Foroosh H. In-band sub-pixel registration of wavelet-encoded images from sparse coefficients. *Signal, Image and Video Processing* 2017; 11 (8): 1527-1535. doi: 10.1007/s11760-017-1116-5
- [34] Aydin VA, Foroosh H. Motion compensation using critically sampled dwt subbands for low-bitrate video coding. In: *IEEE 2017 International Conference on Image Processing*; Beijing, China; 2017. pp. 21-25. doi: 10.1109/ICIP.2017.8296235
- [35] Wang Z, Bovik AC, Sheikh HR, Simoncelli EP. Image quality assessment: from error visibility to structural similarity. *IEEE Transactions on Image Processing* 2004; 13 (4): 600-612. doi: 10.1109/TIP.2003.819861